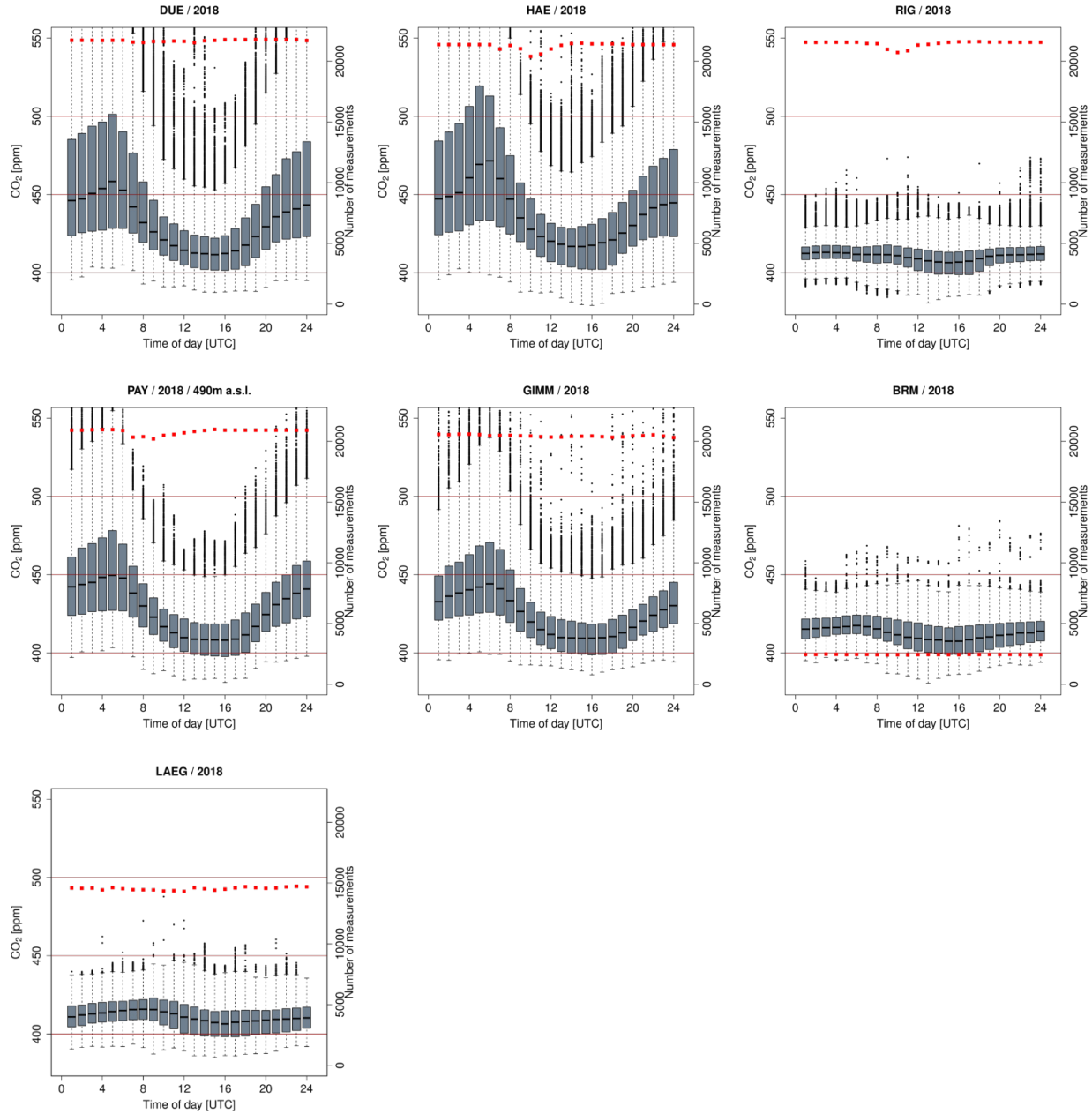Atmospheric
Measurement
Techniques

Supplement of

Integration and calibration of non-dispersive infrared (NDIR) CO_2 low-cost sensors and their operation in a sensor network covering Switzerland

Michael Müller et al.

Correspondence to: Christoph Hüglin (christoph.hueglin@empa.ch)

1 CO₂ molar fraction at sites equipped with high-precision instruments

Figure 1: Boxplots of CO₂ molar fraction referring to time of day observed at sites equipped with high-precision instruments in the year 2018. At BRM the air is probed sequentially at five different heights. Therefore, the number of measurements is smaller than for the other sites. Here, molar fraction from probing in 12 m height is shown. The locations of the sites are depicted in Figure 1 of the publication.

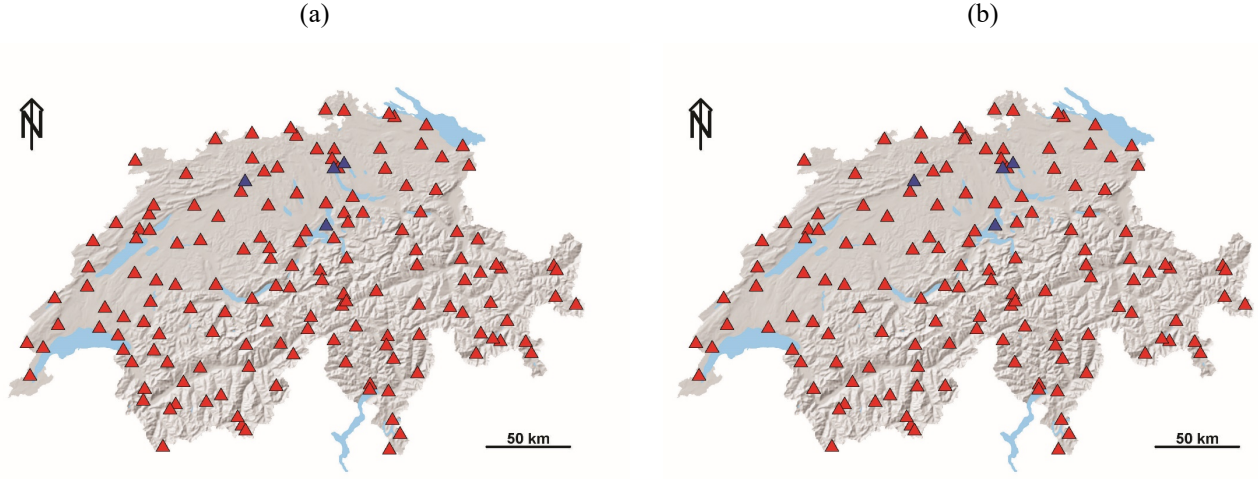## 2 Locations of MeteoSwiss SwissMetNet sites

(a)

(b)

Figure 2: MeteoSwiss SwissMetNet sites (red triangles) and sites of the Swiss National Air Pollution Monitoring network (blue triangles) providing measurements of (a) wind speed and wind direction, and (b) pressure.

3 Comparison of meteorological measurements derived by the sensor units and by instruments of MeteoSwiss SwissMetNet sites

3.1 Computation of the mole fraction of H_2O

The water vapour saturation pressure p_σ is computed by following formula (Wagner & Pruß, 2002)

$$p_\sigma = p_c \cdot e^{\left(\frac{T_c}{T}\left(a_1 \cdot \vartheta + a_2 \cdot \vartheta^{1.5} + a_3 \cdot \vartheta^3 + a_4 \cdot \vartheta^{3.5} + a_5 \cdot \vartheta^4 + a_6 \cdot \vartheta^{7.5}\right)\right)}$$

Here, p_c is the critical pressure of water (22064000 Pa), T_c is the critical temperature of water (647.096 K), T is the temperature (K), and ϑ equals $(1-T_c/T)$. The coefficients a_1 to a_6 have the values: a_1=-7.859 517 83, a_2=1.844 082 59, a_3=-11.786 649 7, a_4=22.680 741 1, a_5=-15.961 871 9 and a_6=1.801 225 02.

The water vapour pressure p_w is obtained by p_σ and the relative humidity RH [%].

$$p_w = \frac{RH \cdot p_\sigma}{100}$$

The mole fraction of H_2O in [%] is computed by

$$\chi_{H2O} = \frac{p_w}{p} \cdot 100$$

3.2 Comparison of temperature and relative humidity from the Sensirion SHT21 sensors and from instruments of the MeteoSwiss SwissMetNet sites
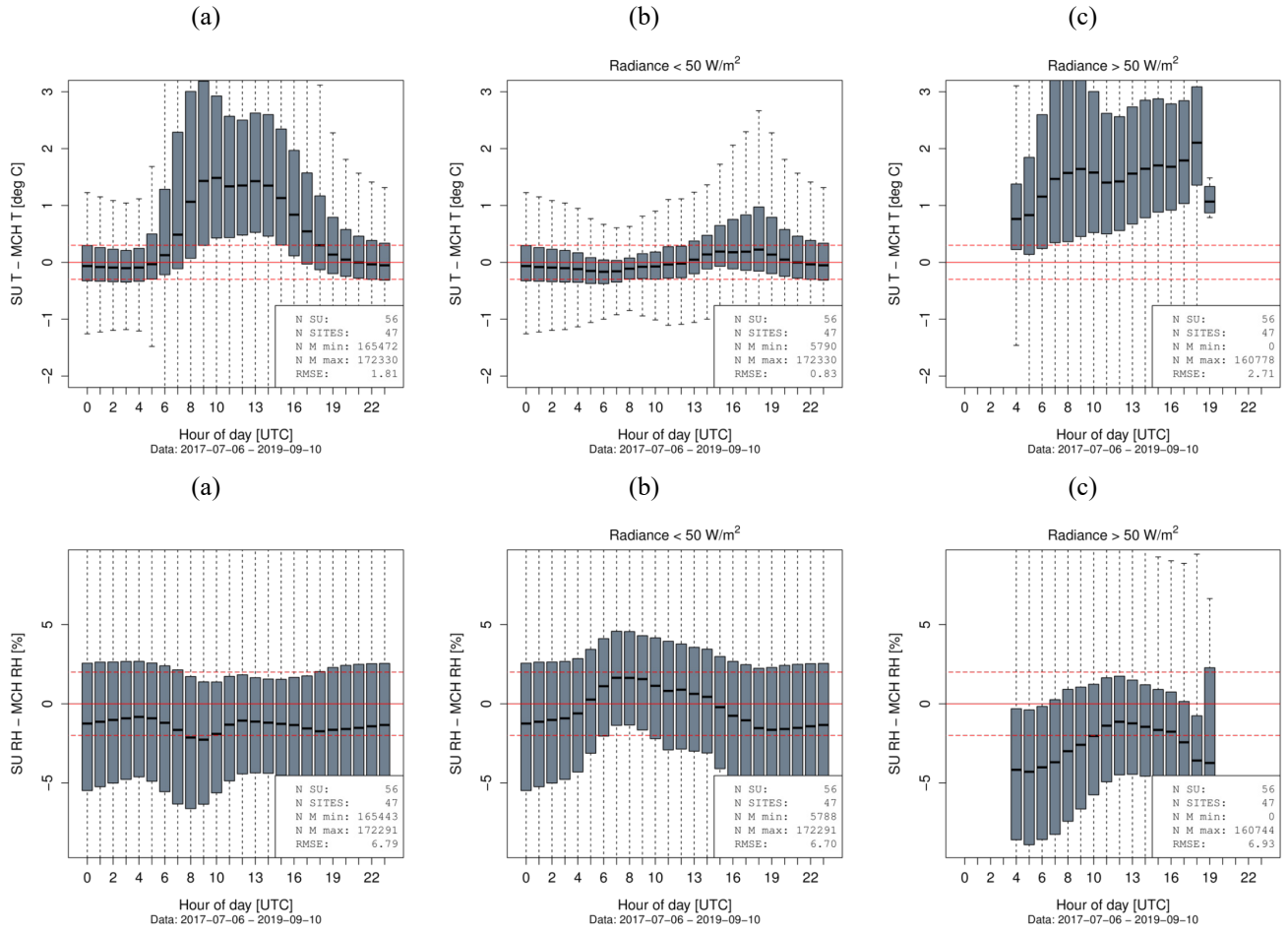

Figure 3: Comparison of temperature (first row) and relative humidity (second row) between the SHT21 sensor within the sensor unit (located at 9.5 m above ground) and the instruments at the MeteoSwiss SwissMetNet sites (located at 2 m above ground). (a) Comparison based on all measurements. (b) Comparison based on the measurements when global radiation is below 50 W/m^2. (c) Comparison based on the measurements when global radiation is above 50 W/m^2. The dashed horizontal lines depict the accuracy of the SHT21 sensor for T (±0.3ºC) and RH (±2%).

3.3 Comparison of water molar fraction computed for the sensor units and computed from reference measurements of the MeteoSwiss SwissMetNet sites
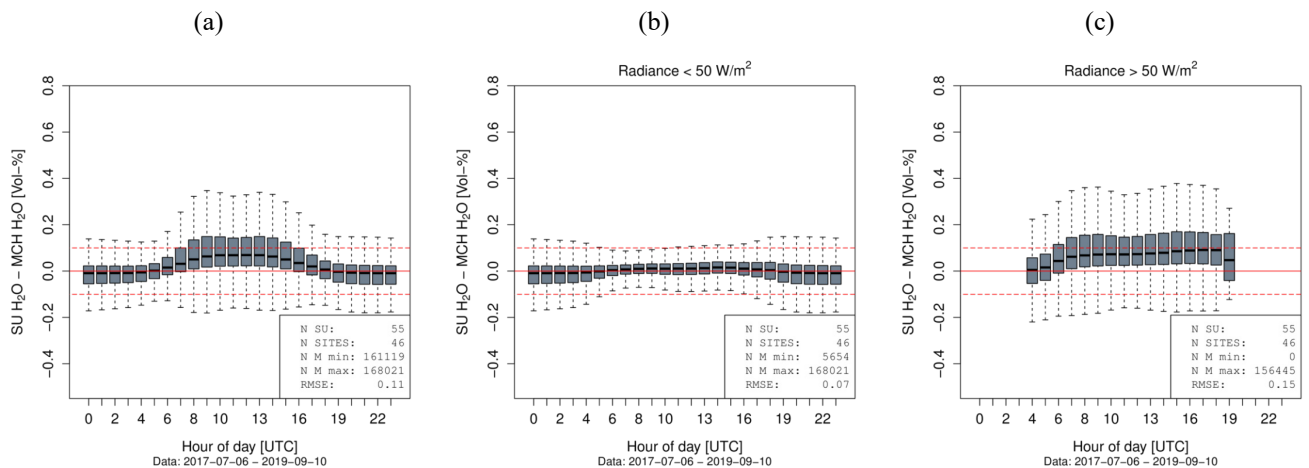
Figure 4: Comparison of the water volume fraction computed based on measurements from the SHT21 sensor (T/RH) and the interpolated pressure and the water volume fraction computed from reference measurements at the MeteoSwiss SwissMetNet sites. (a) Comparison based on all measurements. (b) Comparison based on the measurements when global radiation is below 50 W/m^2. (c) Comparison based on the measurements when global radiation is above 50 W/m^2. The dashed horizontal lines depict the ±0.1%-level.

3

4   Differences between measurements from HAE and DUE depending on options for measurement filtering
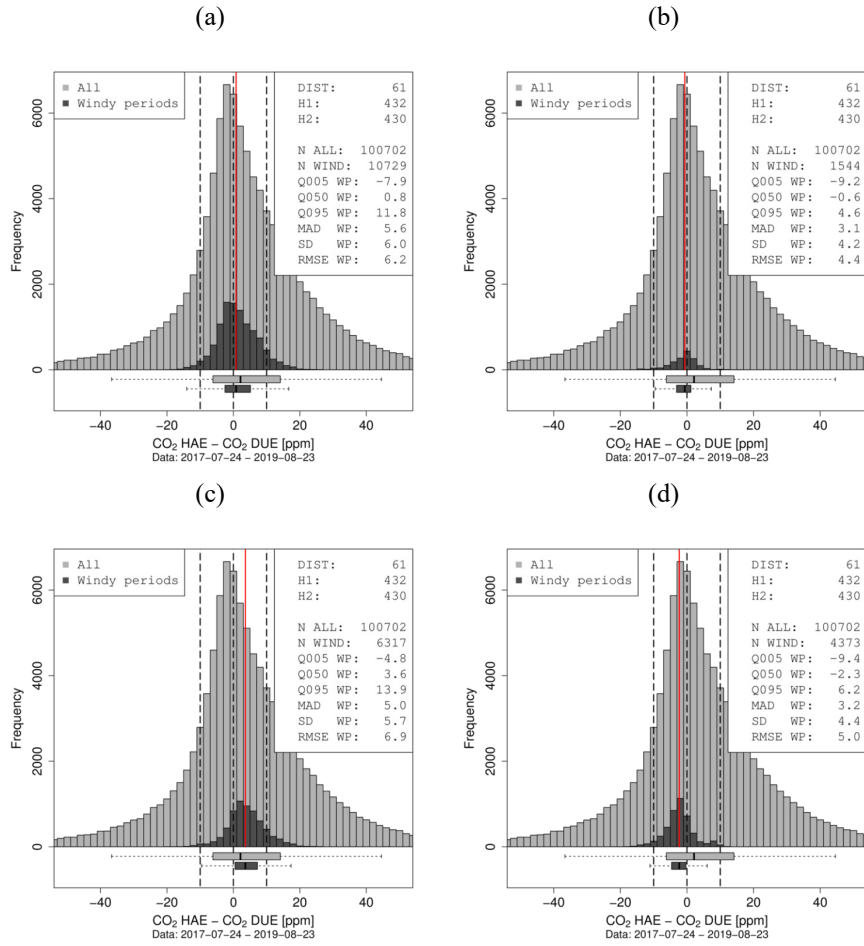
(a)

(b)

(c)

(d)

Figure 5: Differences of 10 minutes CO₂ molar fractions between HAE and DUE. The histogram in light gray refers to all measurements and the histogram in dark grey refers to the measurements (a) in windy conditions, (b) in windy conditions between 22:00 and 04:00 UTC, (c) in windy conditions and wind directions between 80° to 280° (downwind the motorway) and (d) in windy conditions and wind directions between 0° and 80° / 280° and 360° (upwind the motorway). DIST denotes the distance between the two sites [km], H1 and H2 denote the altitudes of the two sites [m]. Q005 WP, Q050 WP, Q095 WP denote the 5%, 50% and 95% quantile of the CO₂ differences in windy conditions. MAD WP and SD WP denote the median absolute deviation and standard deviation of the CO₂ differences in windy conditions. RMSE WP denotes the RMSE of the CO₂ concentrations of the two sites in windy conditions.

5   Comparison between LP8 sensors and high-precision instruments

Figure 6: Comparison of CO₂ from LP8 sensors and from the high-precision instrument at HAE. The LP8 sensor processing based on Eq. (4) and (5) includes the application of the outlier detection algorithm, drift correction and consistency check. Points in grey are flagged as outliers.
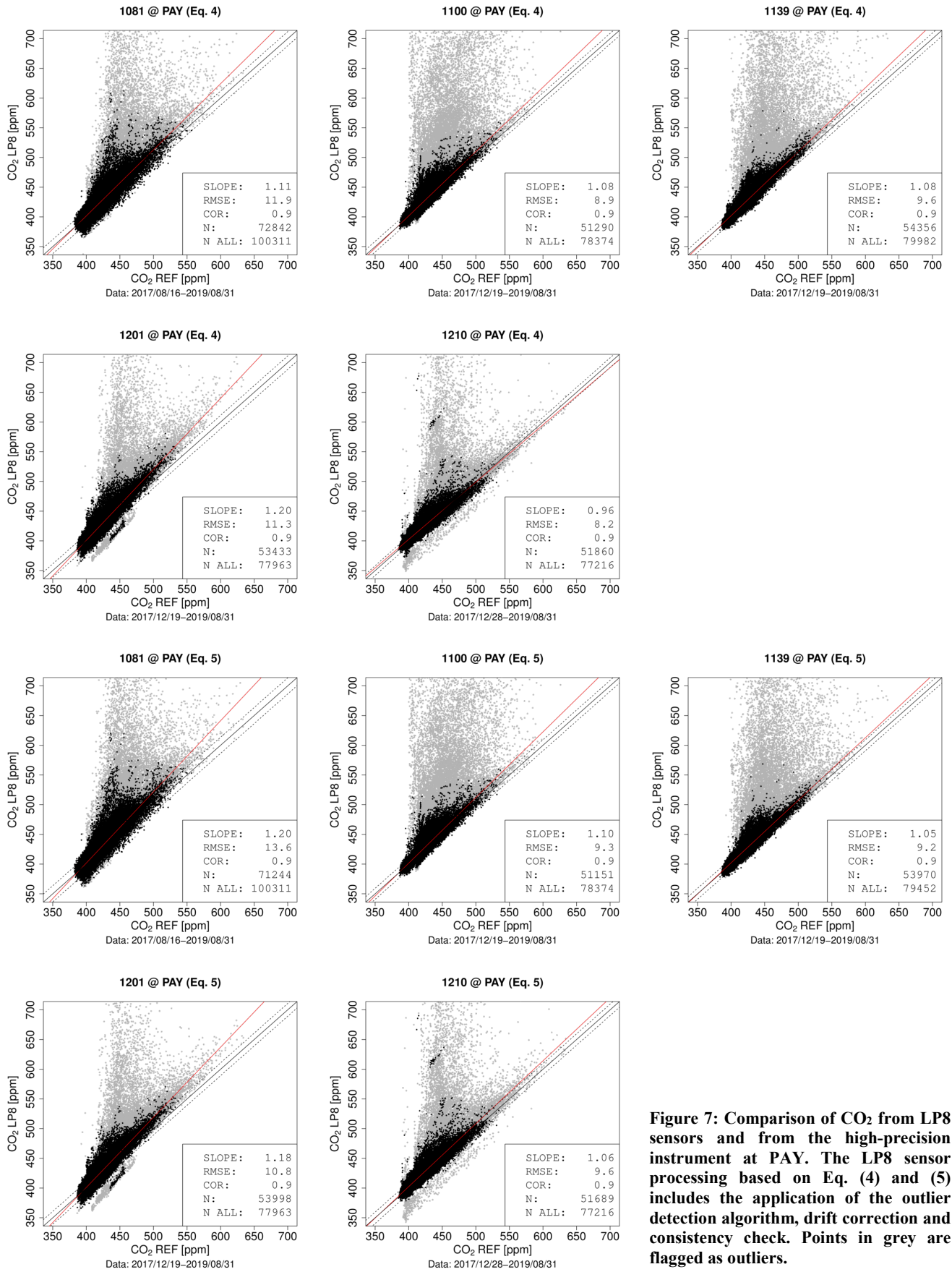
Figure 7: Comparison of CO₂ from LP8 sensors and from the high-precision instrument at PAY. The LP8 sensor processing based on Eq. (4) and (5) includes the application of the outlier detection algorithm, drift correction and consistency check. Points in grey are flagged as outliers.
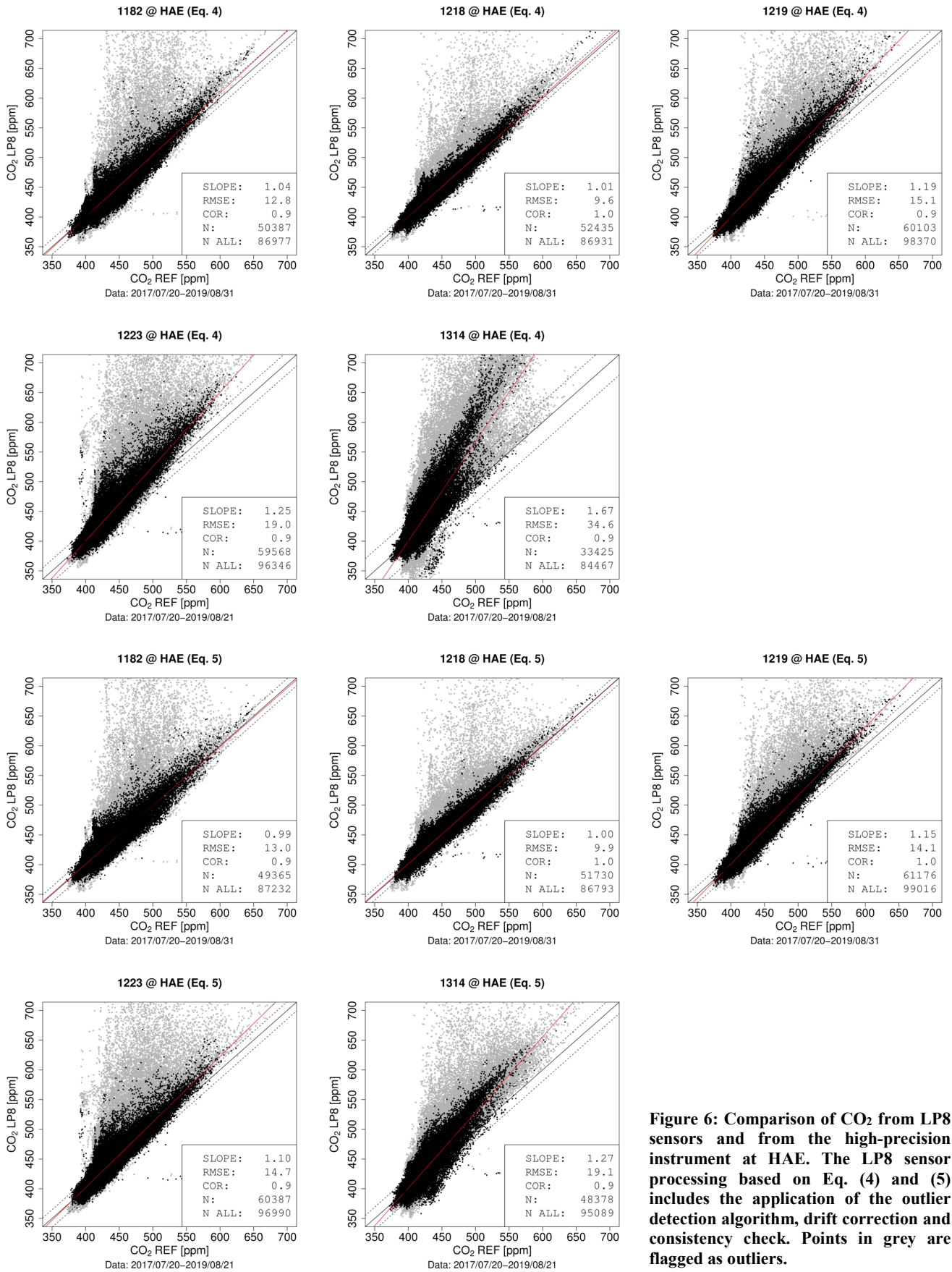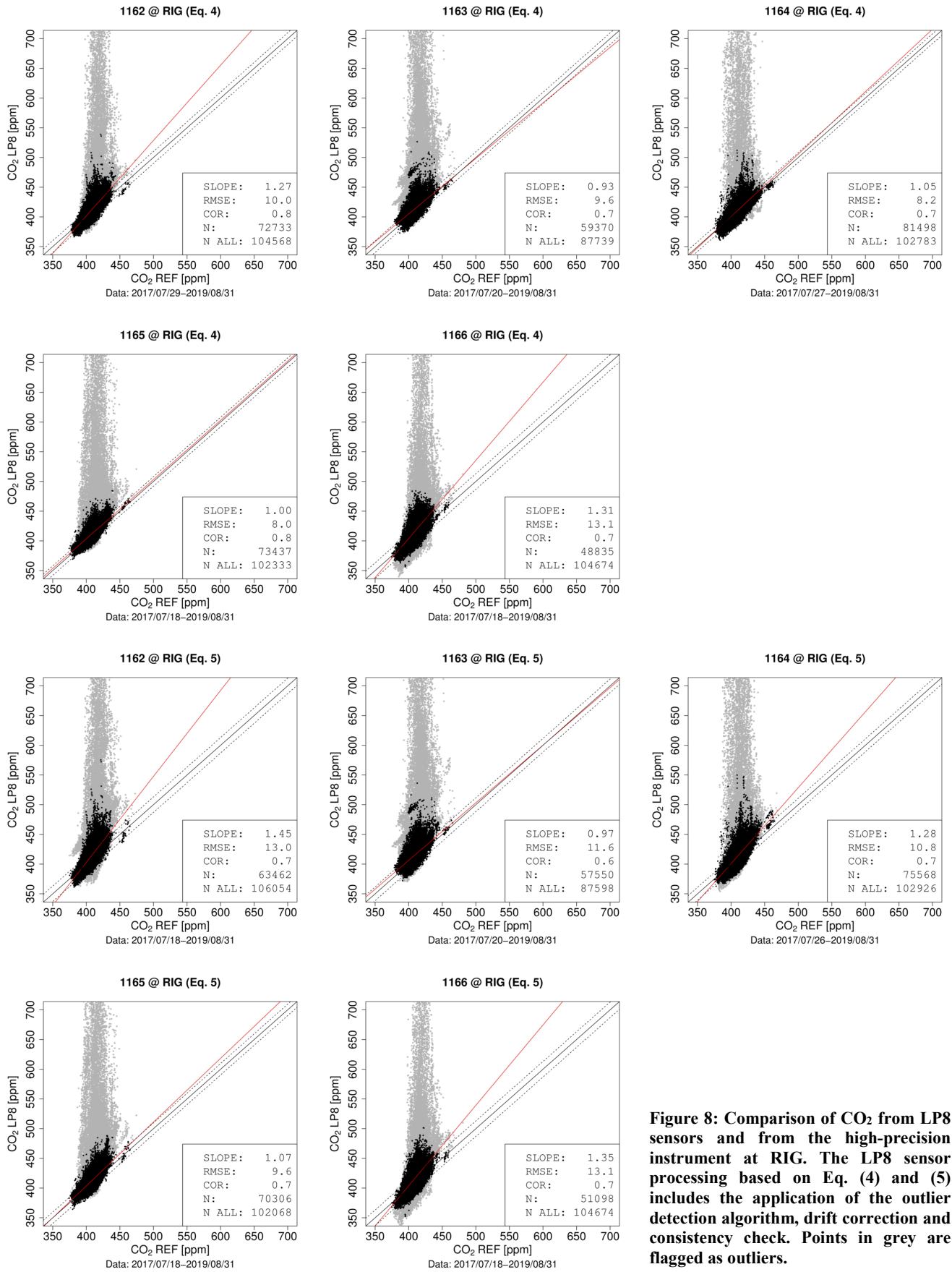
Figure 8: Comparison of CO_2 from LP8 sensors and from the high-precision instrument at RIG. The LP8 sensor processing based on Eq. (4) and (5) includes the application of the outlier detection algorithm, drift correction and consistency check. Points in grey are flagged as outliers.
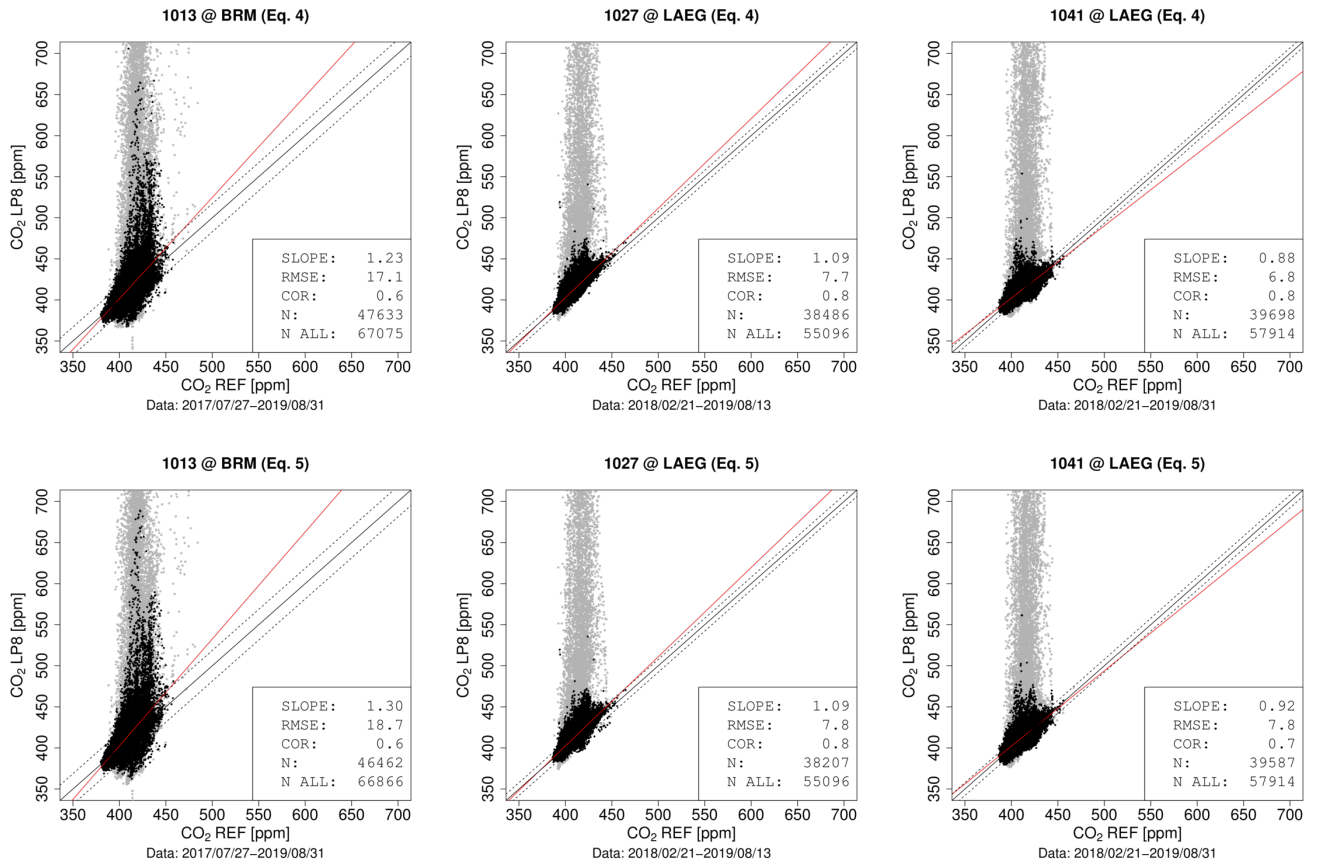
Figure 9: Comparison of CO₂ from LP8 sensors and from the high-precision instrument at BRM and LAEG. The LP8 sensor processing based on Eq. (4) and (5) includes the application of the outlier detection algorithm, drift correction and consistency check. Points in grey are flagged as outliers.

6 Differences between co-located sensors
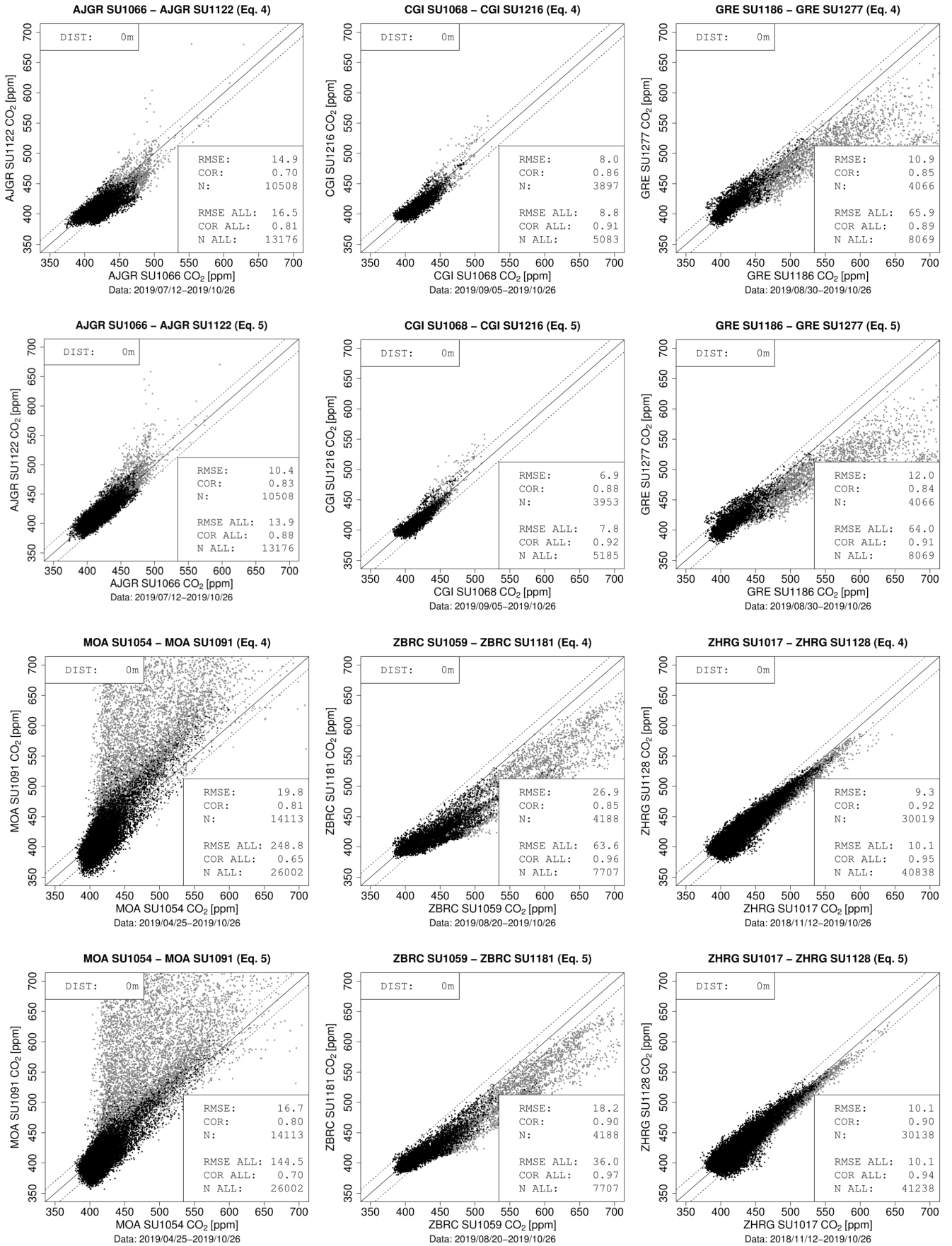
Figure 10: Comparison of LP8 measurements (drift corrected, outlier detection algorithm) from co-located sensors (distance between sensors 0 m). Points in grey are flagged as outliers. The header of the individual figures indicates the sensor pairs by the location name and the sensor unit ID as well as the sensor model.

7   Assessment of the performance of sensors that were replaced in the Carbosense network

(a)

1012 @ DUE (Eq. 5)

SLOPE:	1.28
RMSE:	23.8
COR:	0.9
N:	5364
N ALL:	8475

Data: 2019/08/05–2019/10/26

HLL: 2017-07-06 – 2019-07-23
DUE: 2019-08-05 – 2019-10-26

(b)

1141 @ DUE (Eq. 5)

SLOPE:	0.81
RMSE:	21.1
COR:	0.8
N:	34257
N ALL:	49115

Data: 2018/09/18–2019/10/26

BRL: 2017-10-17 – 2018-09-12
DUE: 2018-09-18 – 2019-10-26

(c)

1173 @ DUE (Eq. 5)

SLOPE:	1.10
RMSE:	13.5
COR:	1.0
N:	34311
N ALL:	44879

Data: 2018/09/12–2019/10/26

VIS: 2017-09-07 – 2018-08-28
DUE: 2018-09-12 – 2019-10-26

(d)

1179 @ DUE (Eq. 5)

SLOPE:	0.56
RMSE:	35.2
COR:	0.5
N:	30367
N ALL:	41202

Data: 2018/11/12–2019/10/26

SMHK: 2017-07-19 – 2018-11-12
DUE: 2019-11-12 – 2019-10-26

(e)

1223 @ DUE (Eq. 5)

SLOPE:	1.11
RMSE:	15.0
COR:	1.0
N:	4725
N ALL:	6159

Data: 2019/08/22–2019/10/26

HAE: 2017-07-20 – 2019-08-21
DUE: 2019-08-22 – 2019-10-26

(f)

1278 @ DUE (Eq. 5)

SLOPE:	1.11
RMSE:	9.7
COR:	1.0
N:	36970
N ALL:	47529

Data: 2018/10/02–2019/10/26

LKBD: 2017-09-08 – 2018-09-12
DUE: 2018-10-02 – 2019-10-26

(g)

1314 @ DUE (Eq. 5)

SLOPE:	1.33
RMSE:	23.1
COR:	0.9
N:	3867
N ALL:	6266

Data: 2019/08/22–2019/10/26

HAE: 2017-07-20 – 2019-08-21
DUE: 2019-08-22 – 2019-10-26

(h)

1326 @ DUE (Eq. 5)

SLOPE:	1.14
RMSE:	14.2
COR:	1.0
N:	11349
N ALL:	13260

Data: 2019/06/24–2019/10/26

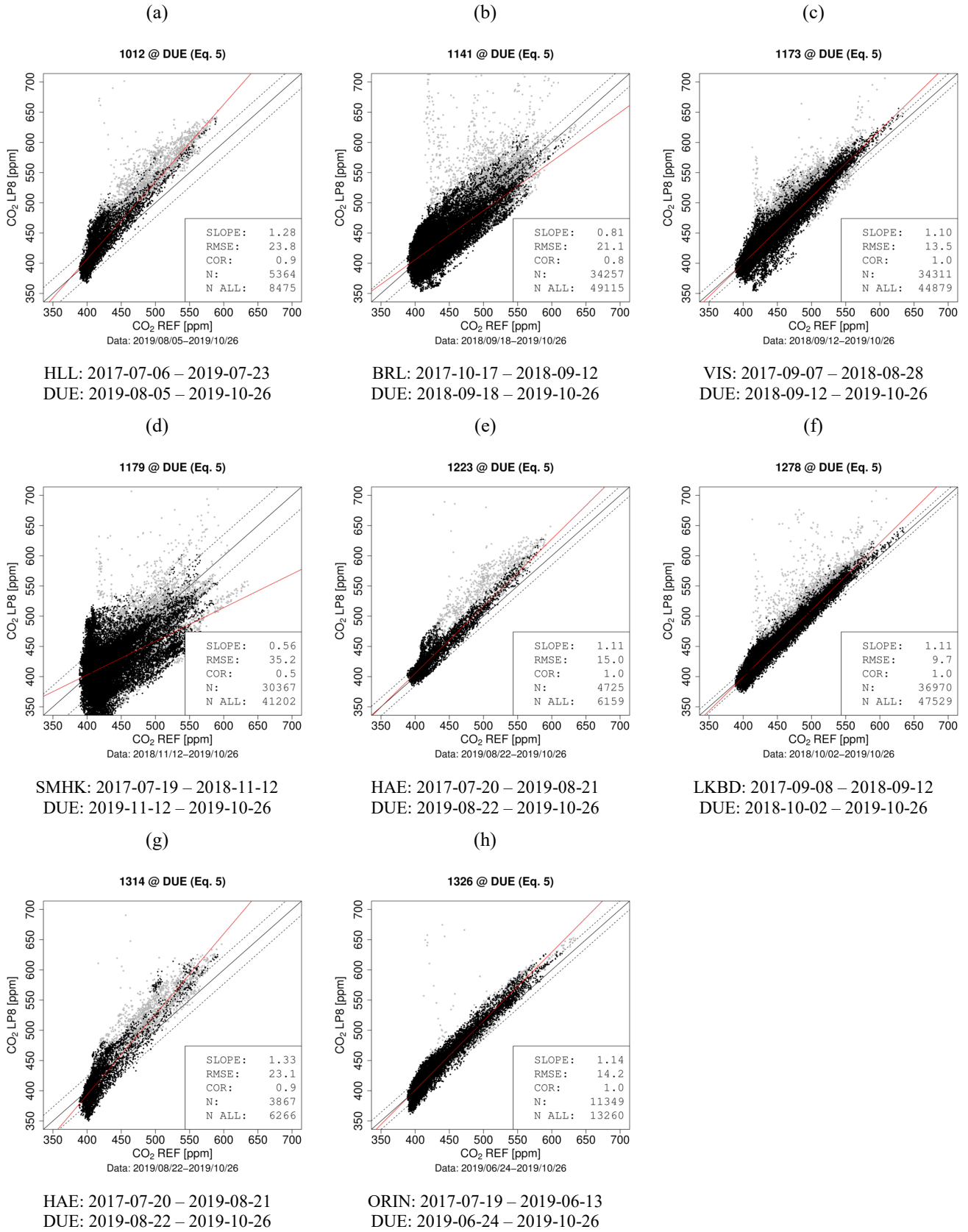ORIN: 2017-07-19 – 2019-06-13
DUE: 2019-06-24 – 2019-10-26

Figure 11: Performance of sensors that were deployed within the Carbosense network for a limited time period and were brought back to site DUE for review their performance. The sensors were replaced in the network due to malfunctioning (e.g. LP8 sensor fell out the board) or suspicious CO₂ measurements. The measurements were processed based on Eq. 5.

8 References

Wagner, W. and Pruß, A.: The IAPWS Formulation 1995 for the Thermodynamic Properties of Ordinary Water Substance for General and Scientific Use. Journal of Physical and Chemical Reference Data, Volume 31, pp. 387-535., 2002.